fibers

MDPI

Article

Influence of Encapsulation Size and Textile Integration Techniques on the Wash Durability of Textiles with Integrated Electronic Yarn

Arash M. Shahidi [1,*], Parvin Ebrahimi [1], Kalana Marasinghe [1], Tharushi Peiris [1], Zahra Rahemtulla [2], Carlos Oliveira [1], Dominic Eberl-Craske [3], Tilak Dias [1] and Theo Hughes-Riley [1,*]

[1] Advanced Textiles Research Group, Nottingham School of Art and Design, Nottingham Trent University, Waverley Building, Waverley Street, Nottingham NG7 4HF, UK; parvin.ebrahimi2022@my.ntu.ac.uk (P.E.); kalana.marasinghe@ntu.ac.uk (K.M.); thelge.peiris2023@my.ntu.ac.uk (T.P.); jose.oliveira@ntu.ac.uk (C.O.); tilak.dias@ntu.ac.uk (T.D.)

[2] Department of Sports Science, School of Science & Technology, Nottingham Trent University, Nottingham NG11 8NS, UK; zahra.rahemtulla@ntu.ac.uk

[3] Imaging Suite, School of Science & Technology, Nottingham Trent University, Clifton Lane, Nottingham NG11 8NS, UK; dominic.eberl-craske@ntu.ac.uk

* Correspondence: arash.shahidi@ntu.ac.uk (A.M.S.); theo.hughes-riley@ntu.ac.uk (T.H.-R.)

Highlights

What are the main findings?

- The wash durability of electronic yarns was systematically evaluated across different textile integration techniques (woven, embroidered, and integrated-knit) and protective micro-pod encapsulation diameters (1.5, 2.0, 3.0, and 6.0 mm).
- Electronic yarns exhibited good durability to machine washing. Only seven of the ninety samples failed during the 25 wash testing cycles. Five failures could be attributed to manufacturing defects.

What is the implication of the main finding?

- These results demonstrate the importance of consistent manufacturing standards when creating reliable, durable, electronic textiles.
- The findings support the development of more durable, application-specific wearable electronic textiles.

Abstract

A crucial factor when developing e-textiles is ensuring their robustness and functionality during everyday activities, particularly washing. The ability to launder e-textile garments is not merely a matter of convenience but a necessity for widespread adoption. Incorporating electronics into textiles can lead to damage due to mechanical and chemical stresses, which most electronics are not designed to withstand. This work focuses on electronic yarn technology (e-yarn), in which electronic functionality is added to textiles by embedding small electronic components into a flexible yarn-like structure. First, the component is soldered onto thin conductive wires. The soldered component is then enclosed in a protective polymer resin (micro-pod). Micro-pods have different diameters depending on the size of the embedded electronic component. The ensemble is finally covered in a textile sheath. This study focuses on the wash durability of e-yarns integrated with textiles in three different ways: embroidered onto the surface of a woven fabric, within a knitted channel in a knitted fabric, and woven as a weft yarn. Further, the work studied the impact of using different sizes of micro-pods on the e-yarns' wash durability. Ultimately, good wash durability was observed under all testing conditions.

check for updates

Academic Editor: Martin J. D. Clift

Received: 6 May 2025
Revised: 10 June 2025
Accepted: 27 June 2025
Published: 2 July 2025

Citation: Shahidi, A.M.; Ebrahimi, P.; Marasinghe, K.; Peiris, T.; Rahemtulla, Z.; Oliveira, C.; Eberl-Craske, D.; Dias, T.; Hughes-Riley, T. Influence of Encapsulation Size and Textile Integration Techniques on the Wash Durability of Textiles with Integrated Electronic Yarn. *Fibers* **2025**, *13*, 89. https://doi.org/10.3390/fib13070089

Keywords: electronic textiles; e-textiles; smart textiles; textile testing; wash durability; washing

1. Introduction

While regular textiles can withstand machine washing, integrating electrical components presents a unique challenge due to their susceptibility to damage from wetting, chemical degradation, and structural stability [1–3] as a result of flexing and abrasion during washing cycles. This work explores the wash durability of electronic textiles (e-textiles) that have been created using electronic yarn (e-yarn) technology. E-textiles have seen significant progress in recent years, in which electronic functionality has introduced new features to traditional textiles [4–6]. The growth of e-textiles has been well-documented in recent literature, with advancements in conductive materials, flexible electronics, and integration techniques driving their adoption in various applications, from healthcare to fashion [7]. One of the most crucial aspects of these advancements is ensuring the durability and functionality of e-textiles during everyday processes, particularly washing. The ability to wash e-textile garments is essential for many applications, and the ability to wash e-textiles using normal washing techniques is essential to consumer acceptance in many areas, and therefore to the widespread adoption of the technology [2,3,6,8].

The wetting, flexing, chemical exposure (detergent) and abrasion experienced by textiles during a machine-washing cycle introduce durability challenges for the embedded electronics [9,10]. To mitigate these issues, recent research has focused on developing protective coatings, robust encapsulation methods, and novel material designs with some success. For example, studies by Ojstršek et al. (2022) [11] have reviewed the use of the dip-coating technique, highlighting its impacts on functionality, durability, and sustainability. Also, Liman et al. (2022) [12] presented a comprehensive review on the current state of the art in washable e-textile designs, focusing on innovative strategies such as unique textile geometries, encapsulation, adhesion behavior, self-repairability, and standardized washing protocols to address common washing stresses. These approaches have shown promising results in extending the lifespan and functionality of e-textiles [11,13–15]. Given the diversity of methods used to incorporate electronics within textiles, wash durability remains an ongoing area of investigation for many researchers [3,8,16,17]. This work focuses on the wash durability of e-yarns, where electronics are embedded within the core of textile yarns, which are then incorporated into textiles. The technology has been applied to a disparate range of applications, including fall and near-fall detection [18,19] and solar energy harvesting [20,21]. The production process begins with soldering a small-scale commercial component (in this study, a 10 kΩ resistor) onto fine, flexible, multistrand litz wires with an overall diameter of approximately 250 µm. This step ensures a robust electrical and mechanical connection between the wire and the component. To enhance the durability of the ensemble, the solder joints and component(s) are encapsulated within a rigid resin micro-pod, which is slightly larger than the component itself. Encapsulation is crucial for safeguarding electronic components within e-yarns, preserving their durability, performance, and resistance to mechanical stress and moisture exposure during washing [22–24]. Supporting yarns running parallel to the litz wires are added at this stage to create a uniform cross-section and improve the mechanical strength. Finally, the wires and encapsulated device are embedded within a cylindrical textile structure, typically a braid, which provides additional stability and protection, and aids in the processability of the final device [25].

A previous wash durability study, using e-yarns from 2020, highlighted durability issues during the machine-washing process, particularly at the wire–micro-pod interface,

where significant mechanical stresses resulted in failure of the wire [26]. Due to this, and to other issues identified with the e-yarn, a new design was created which is believed to be significantly more durable [21].

Given the variety of applications and diverse end-user requirements for e-textiles, understanding the effect of the integration process for the e-yarn within a textile is essential. Hence, this study investigated the durability of e-yarns embedded into three types of e-textiles: where the e-yarn was embroidered onto the surface of a woven fabric, embedded within a knitted channel structure (integrated-knit), and woven as a weft yarn within a woven fabric. It was believed that the incorporation method would significantly impact the e-yarn's resilience to mechanical stress and washing [2,27]. Each textile structure presents distinct advantages and challenges in maintaining durability [16]. Embroidered e-yarns, positioned on the fabric surface, are more susceptible to mechanical wear during use and washing [8]. In contrast, embedding e-yarns within a knitted channel enhances flexibility and stretchability, improving comfort, but exposing the yarns to more significant mechanical stress. Woven e-yarns could offer the highest level of stability and protection, as they are securely enclosed within the fabric structure, minimizing exposure to external forces. This study seeks to deepen the understanding of these integration techniques by evaluating their impact on wash durability. The findings will provide valuable insights into optimizing e-yarn-embedded e-textile design for improved longevity in real-world applications. In addition, this knowledge may hold value for other academics working on yarn-type electronic integrated devices [28].

Previous research has indicated that the size of the micro-pod used for the component encapsulation has had an influence on the e-yarn durability [26]. Therefore, this study has also investigated different micro-pod dimensions. Each e-yarn type requires a different micro-pod size, depending on the component being embedded. To ensure the consistency and comparability of results with those of other researchers, this study adheres to a recognized washing standard, BS EN ISO 6330:2021 (Domestic Washing and Drying Procedures for Textile Testing [29]). ISO 6330 was previously used by researchers in an earlier study and has also been employed by other e-textile researchers in evaluating the durability of e-textiles [26,30–32]. The standards define specific washing and drying cycles that simulate real-world laundering conditions. Ultimately, it is desirable for e-textiles to be durable under normal washing conditions; hence, a standard developed for conventional textile fabrics has been used [3]. By following this standard in the present work, the findings of the study can be made relevant and applicable to practical use cases and the credibility and reliability of the study can be enhanced.

This study underscores the importance of wash testing for e-textiles, specifically, those made using e-yarns, and the necessity of studying their robustness and functionality throughout the usual wash cycles. Key factors, including the micro-pod size and method of e-yarn integration, were explored to understand their effect on the durability of e-yarns. The findings are expected to advance the field of e-textiles by providing a deeper understanding of the durability and performance of e-yarns given different integration methods and micro-pod sizes.

2. Materials and Methods

2.1. Electronic Textile Preparation

To investigate the e-yarns durability under repeated wash test cycles, 90 samples were prepared (Table 1). The e-yarns were first created by soldering 10 kΩ SMD resistors (10 kΩ resistor part number: CRCWO40210KOFKED, Vishay Intertechnology, Malvern, PA, USA) onto two litz wires (BXL2001, OSCO Ltd., Milton Keynes, UK), using a hand soldering process (AX25 soldering iron, Antex Electronics, Plymouth, UK) and Lead Free RS PRO

soldering wire (0.25 mm and 228 °C melting point). Resistors were selected for testing because any damage to the conductive litz wires during washing or disconnection from the component can be clearly identified through a resistance measurement.

Table 1. Summary of the numbers of samples prepared for this work. 'E' denotes encapsulation, followed by the encapsulation size in millimeters (e.g., E1.5 = 1.5 mm encapsulation). The 'P' suffix (e.g., E1.5P) indicates comparative samples prepared independently by a second researcher, using the same encapsulation size.

Encapsulation Naming Code	Encapsulation Size (mm)	Woven Samples	Embroidered Samples	Integrated-Knit Samples	Total Samples
E1.5	1.5	10	10	8	28
E1.5P	1.5	6	6	5	17
E2	2	5	5	5	15
E3	3	5	5	5	15
E6	6	5	5	5	15
Total		**31**	**31**	**28**	**90**

This assembly was subsequently encapsulated within a micro-pod formed from a commercially available polymer resin (Dymax 9001-E-V3.5; Dymax Corporation, Torrington, CT, USA). The resin had the following properties: UV cure: 30 s; heat cure: 60 min at 110 °C; elongation: 150% at breaking point; hardness: 45 D; tensile strength: 750 psi at breaking point; viscosity: 4500 cP; and volume resistivity: 555 × 10^{12} ohm-cm. Different sizes of encapsulation molds (1.5 mm, 2 mm, 3 mm, and 6 mm), together with four supporting polyester yarns (1/167/48, J. H. Ashworth & Son Ltd., Hyde, UK), were used. This encapsulation was a protective layer, preventing physical and environmental damage while maintaining the e-yarn's functionality. The four sizes were chosen to represent the range from the smallest micro-pod commonly used (1.5 mm, suitable for a 0402 size component such as an LED or thermistor) up to an extreme case larger than any component that would be used in an e-yarn (6 mm). Only cylindrical pods were investigated in this work. For the purposes of sample naming, the encapsulation sizes are denoted E1.5 (1.5 mm diameter micro-pod), E2 (2.0 mm diameter micro-pod), E3 (3.0 mm diameter micro-pod), and E6 (6 mm diameter micro-pod); see Figure 1.

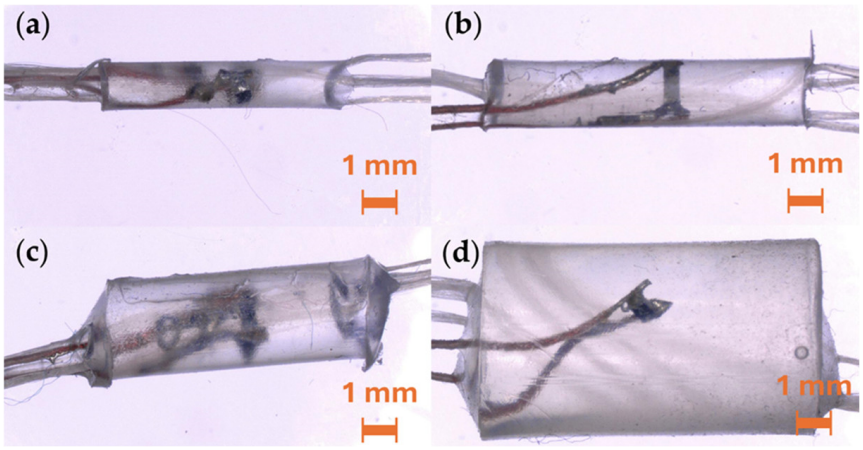

Figure 1. Microscope images of a selection of encapsulated resistors that have been soldered onto litz wire. The encapsulation contains four supporting polyester yarns; 20× magnification. (**a**) 1.5 mm diameter micro-pod (E1.5); (**b**) 2.0 mm diameter micro-pod (E2); (**c**) 3.0 mm diameter micro-pod (E3); (**d**) 6.0 mm diameter micro-pod (E6).

The final structure was consolidated using a Herzog Braiding Machine (Herzog GmbH, Oldenburg, Germany). A crucial factor affecting the structural integrity and flexibility of the braided samples is the lay length, defined as the distance between the crossover points of the braiding yarns. To maintain consistency across all samples, the lay length was set at a constant 7 PPI (picks per inch of length), alongside other key parameters like the use of 2-end polyester yarns (2/167/38, J. H. Ashworth & Son Ltd., Hyde, UK) and 24-yarn carriers, and a machine speed of 250 revolutions per minute. Figure 2 illustrates a diagram of the e-yarn's structure.

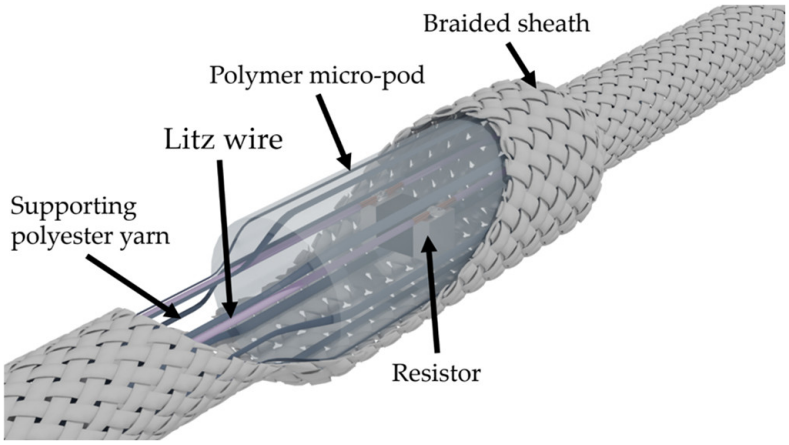

Figure 2. Schematic of an electronic yarn with an embedded resistor.

The final e-textile samples used three integration techniques to embed the e-yarns: weaving, embroidery, and knitting (knitted channel integration technique). All of the textile samples were 100 × 100 mm. Sample codes were amended with "W" for woven, "E" for embroidered, and "K" for integrated knit.

For the woven samples, the e-yarns were incorporated during the fabric production process as supplementary weft yarns. This was accomplished using a hand-operated, computer-controlled Jacquard weaving loom (Thread Controller 2, Digital Weaving Norway, Moss, Norway). The warp was made from polyester (Ne 2/30; John L Brierley Textiles Ltd., Huddersfield, UK), while identical yarns were employed for the weft, with the exception of the e-yarns.

The embroidered samples comprised e-yarns attached to a polyester canvas fabric (Albany; Whaleys Bradford Ltd., Bradford, West Yorkshire, BD7 4EQ, UK), a woven material composed of 100% polyester, and with a weight of 290 GSM. Attachment was achieved using a Bernina 1000 Special sewing machine (BERNINA Textile Group, Steckborn, Switzerland), employing a zig-zag stitch pattern set at a stitch setting of 5 and utilizing a free-hand foot (No. 9). The selection of the zig-zag stitch was deliberate, as it effectively enhances surface contact and ensures the secure anchoring of e-yarns to the fabric base. For optimal outcomes, the stitch width was precisely adjusted for each sample type.

For samples E2 and E6, a stitch width of 4 mm was utilized, whereas samples E3 and E1.5 were stitched with a width of 3 mm. It is important to note that the encapsulated regions of samples E3 and E6 required manual adjustment, which involved lifting the needle foot and manually guiding the fabric to achieve precision and consistency during the embroidery process. To maintain the integrity of the encapsulated regions of the e-yarns, the stitching process was meticulously optimized to ensure consistent tension throughout. This careful optimization prevented any damage to the encapsulated areas while allowing for precise placement of the e-yarns onto the fabric. The resulting embroidery demonstrated strong adhesion between the e-yarns and the substrate while preserving flexibility, thus ensuring the samples' functionality and durability.

For integrated-knit e-textiles, a plain knitted structure was created using four ends of polyester yarn (1/167/48, J. H. Ashworth & Son Ltd., Hyde, UK) and produced with an all-needle interlock double/bed technique on a flat-bed knitting machine (Stoll CMS ADF 32 W E7.2; Reutlingen, Germany). The knitted samples were designed with specialized channels that enabled the secure incorporation of the electronic yarns (e-yarns).

Ten samples for each integration method were produced for the 1.5 mm encapsulation size (E1.5). However, two breakages occurred prior to testing. (A total of 28 samples were tested.) Five samples using the 2 mm (E2), 3 mm (E3), and 6 mm (E6) encapsulation sizes were also produced for each integration technique (45 samples). Finally, a second set of samples using a 1.5 mm encapsulation size was produced by a different researcher with greater experience in soldering small-scale components (denoted as E1.5P; 17 samples in total). This was to study whether variations in the manufacturing of the e-yarns had a significant effect on the overall durability. Table 2 summarizes the sample naming scheme. Microscope images showcasing electronic yarns embedded within textile structures are presented in Figure 3, while details of the dimensions of the electronic components are summarized in Table 3.

Table 2. Sample naming conventions used in this work.

Code Element	Meaning	Example
E	Encapsulation	E2-W
X (2, 3, 6, 1.5 mm)	Encapsulation size	E3-K
XP	Comparative samples by a second researcher	E2P-E
Y	Individual sample number	E6-3
W	Woven integration	E2-W
E	Embroidered integration	E3-E
K	Integrated knit	E1.5-K

Table 3. Electronic component dimensional information.

Electronic Component	Length (mm)	Encapsulated Thickness (mm)	Braided Thickness (mm)	Woven (mm)	Embroidered (mm)	Integrated-Knit (mm)
E1.5	7.42 ± 0.10	1.50 ± 0.04	1.74 ± 0.05	1.95 ± 0.03	2.29 ± 0.05	1.95 ± 0.03
E2	10.02 ± 0.12	2.03 ± 0.04	2.38 ± 0.05	2.51 ± 0.03	2.97 ± 0.03	3.12 ± 0.03
E3	8.20 ± 0.09	3.01 ± 0.03	3.32 ± 0.2	3.48 ± 0.03	3.62 ± 0.03	3.77 ± 0.03
E6	10.45 ± 0.09	5.95 ± 0.04	6.15 ± 0.04	6.2 ± 0.07	6.7 ± 0.07	7.73 ± 0.07

As evident in Figures A1 and A2, the fabric is generally thicker, even in areas where only the e-yarn is present. The point where the encapsulated component is located is even thicker than the base fabric, with the extent of this difference depending on the size of the encapsulation. Furthermore, after integration, the fabric becomes heavier than the base fabric, depending on the size of the encapsulant. The textile thicknesses and weights are provided in Appendix A.

2.2. Washing and Drying Protocol

The washing and drying procedures were conducted in accordance with BS EN ISO 6330:2021 [29], which specifies standard domestic laundering conditions for textiles. The samples were washed with a household front-loading washing machine, Bosch Logixx 8 (BSH Home Appliances Ltd., Milton Keynes, UK), maintaining a total wash load of 2.00 ± 0.01 kg, which included the test samples. Each washing cycle employed 20 g of Persil Non-Bio Washing Powder (Unilever UK Ltd., London, UK) as the detergent.

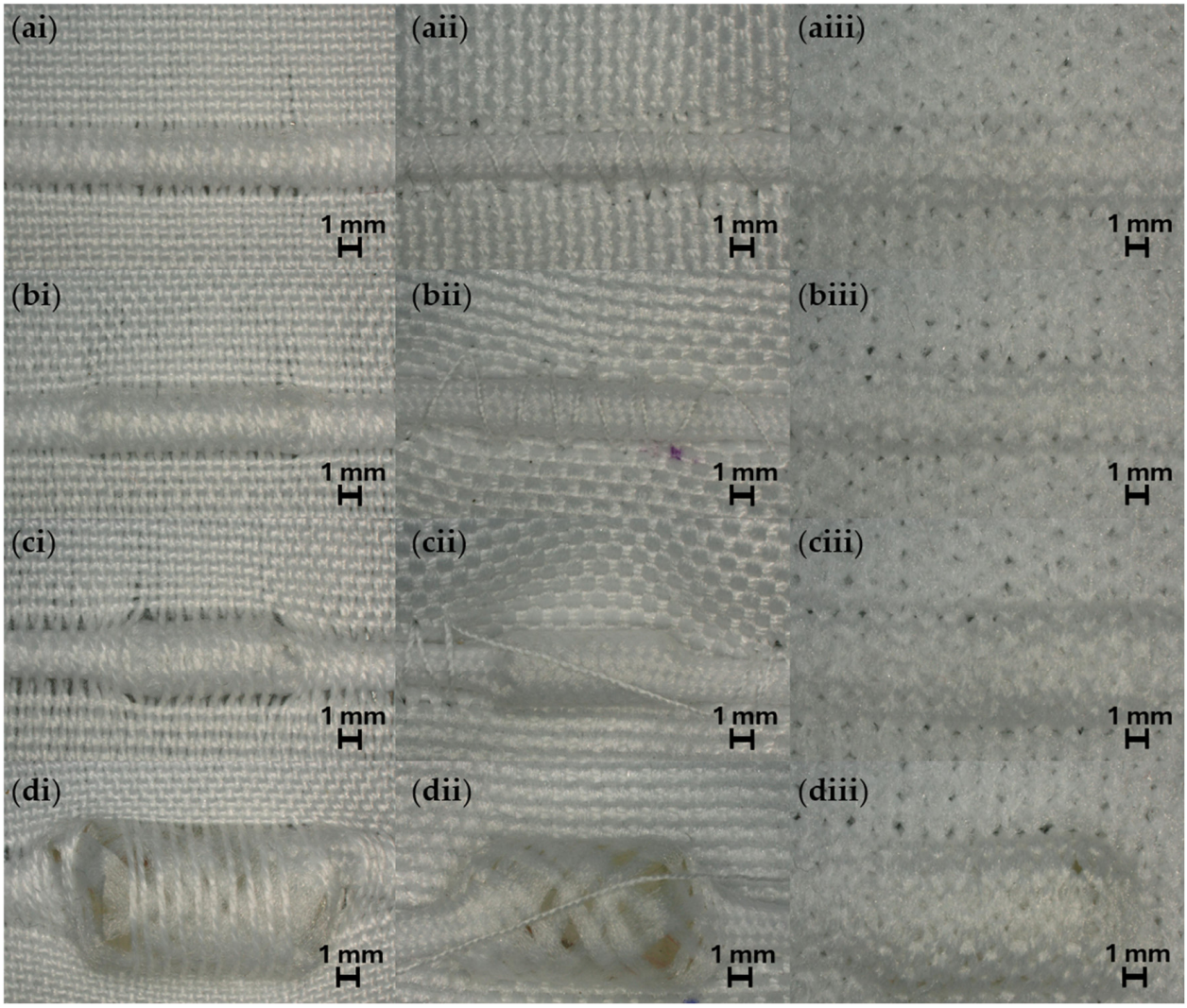

Figure 3. Microscope images of electronic yarns embedded within textile structures. Images focus on the location of the electronic component; 20× magnification. (**a**) 1.5 mm diameter micro-pod (E1.5); (**b**) 2.0 mm diameter micro-pod (E2); (**c**) 3.0 mm diameter micro-pod (E3); (**d**) 6.0 mm diameter micro-pod (E6). (i) woven structure; (ii) embroidered; (iii) integrated-knit.

The washing process consisted of three stages: a 15 min wash at 40 °C, a 10 min rinse, and a 6 min spin cycle at 800 rpm. Preliminary trials were conducted that showed the entanglement of the e-yarn throughout the wash cycles, which led to the decision to use wash bags for protection. Therefore, to prevent entanglement, wash bags were used, with samples from each category placed in separate bags. This is a common practice when conducting wash durability tests with e-textiles; for example, Baribina et al. (2018) [32] and Tadesse et al. (2019) [33] have used wash bags in their own tests. After washing, the samples were air-dried indoors within their wash bags to protect them from any unwanted damage while they were wet; this is shown in Figure 4.

2.3. Microscopy, Mass, and Dimensional Assessments

All visual analyses described in this study were performed with a digital microscope (VHX-5000; Keyence, Osaka, Japan). To address the inherent challenges in achieving consistent measurements under the microscope, which stem from the different integration methods used, all measurements were taken using a digital caliper (Farnell Multicomp Pro, Canal Road, Leeds, LS12 2TU, UK) to ensure precision. Furthermore, all sample sizes and dimensions were recorded after allowing the fabric to rest for 24 h. Mass measurements

were conducted using a precision balance (Adam Equipment PGW 735i, PGW Precision Balance, UK).

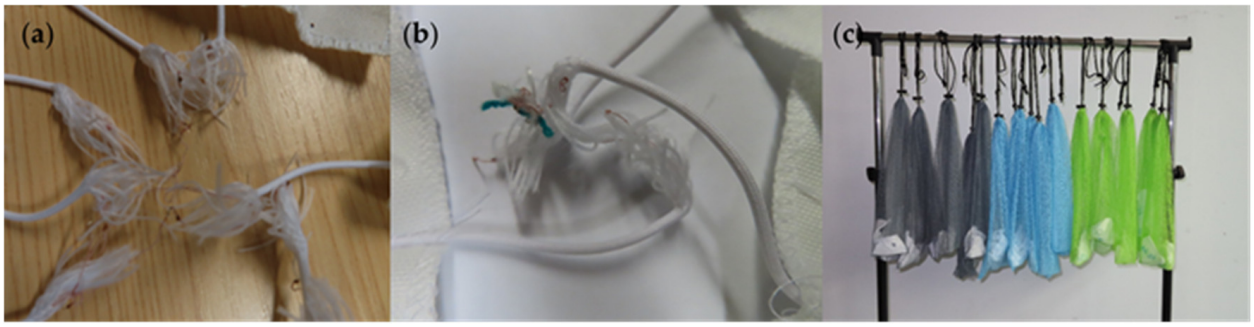

Figure 4. Visual representation of the e-yarn preliminary trials and drying strategy: (**a**) samples before the preliminary wash trial; (**b**) samples after the preliminary wash trial, showing entanglement; and (**c**) the drying process using the wash bag.

2.4. Functional Testing

Failure was determined by measuring the resistance across the e-yarn after each wash cycle (full measurements are provided in the data archive), with failures identified as breaks in electrical continuity. The e-yarns underwent functionality testing during fabrication, before and after integration into the fabric, and after each individual wash test. A benchtop data acquisition unit (Keithley DAQ6510 Data Acquisition and Logging System, Cleveland, OH, USA) was used to record resistance values. This systematic approach allowed for precise tracking of performance degradation over the course of 25 wash–dry cycles.

2.5. Data Processing and Statistical Analysis

Unless otherwise stated, all reported measurements are averages calculated from the individual sample groups; the full set of raw data is available in the data repository. The standard deviation was calculated using the STDEV.P function in Microsoft Excel (Albuquerque, NM, USA). Additionally, percentages are used to represent the proportion of e-yarns that remained functional or failed after the testing process, offering a clear indication of their reliability and durability under the given experimental conditions. This approach ensures a comprehensive performance assessment while accounting for potential sample variations.

2.6. Fault Detection After Failure

Faulty samples were thoroughly examined via X-ray radiography utilizing a Nikon XT H 225 (XT H Series–Nikon Metrology, Belgium), run at a kV peak of 70 kV with a power of 6 W, to identify the underlying causes of failure. This investigation sought to determine whether the failures originated from manufacturing defects, such as poor soldering quality and air bubbles in the encapsulation, or if they were the result of external factors, such as the mechanical stress, flexing, or strain experienced during the wash cycles. By analyzing the internal structure of the samples, weak points and structural vulnerabilities were identified, providing crucial insights into potential areas for improvement. Importantly, the non-destructive nature of this method ensured that the samples did not experience additional damage in the disassembly of the sample (to identify the fault). Non-destructive X-ray radiography enables detailed imaging of internal structures without damage to the samples and allows exhaustive evaluations of the integrity of the material [34,35]. Previous studies have successfully used this method to elucidate the performance of conductive materials in textiles, which demonstrates its reliability and effectiveness in the identification of potential failure points, improving the development of textiles and durable textiles [36–39].

3. Results

3.1. Effect of Encapsulation Size and E-Yarn Integration Technique on the Wash Durability of E-Textiles

The wash durability test results after 25 wash cycles for different integration techniques (woven, embroidered, and integrated-knit) with various encapsulation sizes (E2, E3, E6, E1.5, and E1.5P) are summarized in Figure 5 and detailed in Table 4.

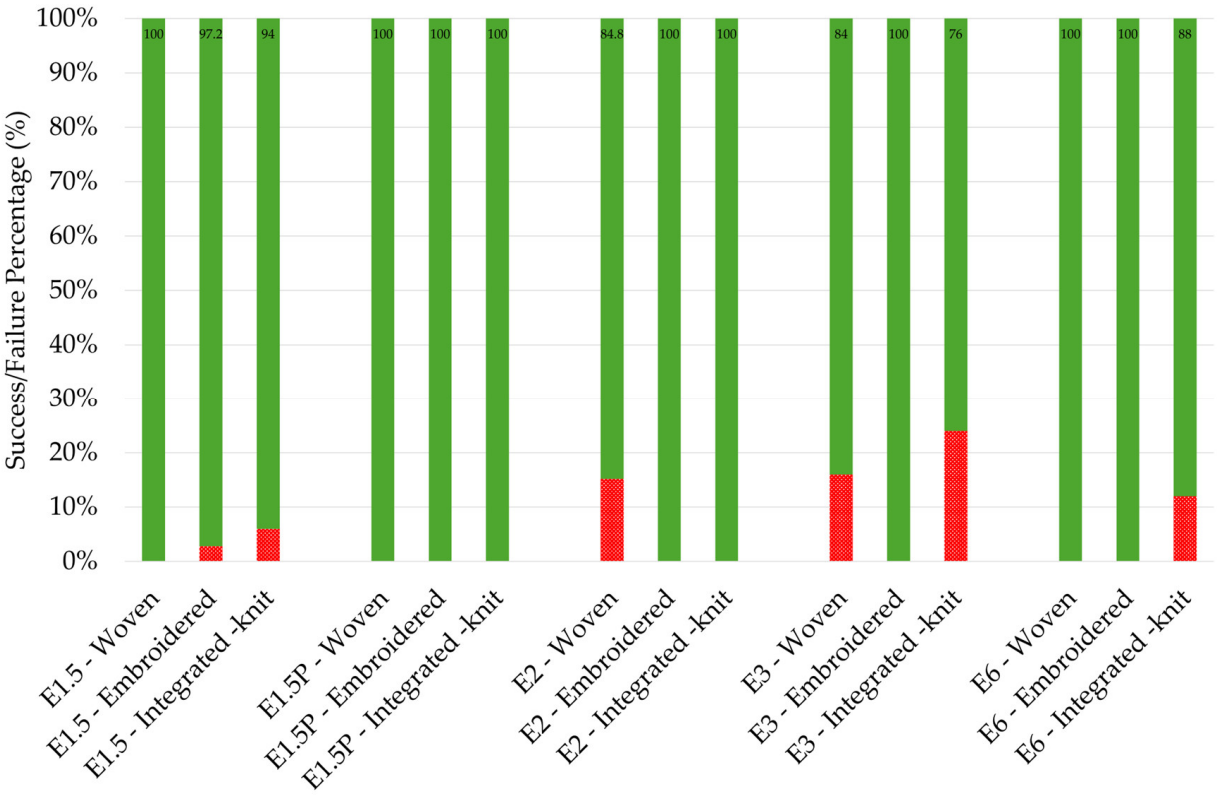

Figure 5. The success and failure rates for wash durability across different fabric integration techniques—woven, embroidered, and integrated-knit—for various encapsulation sizes (E2, E3, E6, E1.5, and E1.5P). The chart visually represents the percentage of successful and failed wash durability tests, with green bars indicating success and red bars indicating failure.

Table 4. Summary of the percentage of e-yarn integrated e-textiles functioning correctly following 25 machine-washing cycles.

Integration Type	E1.5	E1.5P	E2	E3	E6
Woven	100	100	84.8	84	100
Embroidered	97.2	100	100	100	100
Integrated-Knit	94	100	100	76	88

Overall, the e-yarns were observed to be very durable and only seven of the ninety e-yarns broke during the test.

The results reveal the varying performance of the woven fabrics, depending on the encapsulation size. Samples with encapsulation sizes E6, E1.5, and E1.5P demonstrated excellent durability, achieving a 100% success rate with no failures after 25 washing cycles. In contrast, woven fabrics with encapsulation sizes E2 and E3 exhibited slightly lower success rates, at 84.8% and 84%, respectively. This suggested a marginally higher susceptibility to damage or failure for these configurations, which may have been due to limitations in the protective capabilities of the smaller encapsulation sizes or differences in integration techniques.

For the embroidered integration approach, the results were consistently excellent across most encapsulation sizes. Samples with encapsulation sizes E2, E3, E6, and E1.5P achieved a 100% success rate, demonstrating robust performance and strong resistance to washing-induced failures. However, the sample with encapsulation size E1.5 showed a failure rate of 2.8% and achieved a success rate of 97.2%. While this failure rate was relatively small, it may indicate some vulnerability in this particular configuration, possibly due to a slight variation in encapsulation or integration during manufacturing. Notably, the embroidered sample with encapsulation size E1.5P, which another researcher produced to study variations in manufacturing processes, achieved a 100% success rate, underscoring its robustness and reliable performance under washing conditions.

In contrast to the woven and embroidered fabrics, integrated-knit fabrics exhibited more variability in their durability, depending on the encapsulation size. Samples with encapsulation sizes E2 and E1.5P performed exceptionally well, with both achieving a 100% success rate and no recorded failures. Knitted samples with encapsulation sizes E1.5 and E6 displayed slightly lower durability, with 94% and 88% success rates, respectively. While these results still indicate relatively strong performance, the presence of some failures highlights potential challenges in maintaining durability for these configurations. The knitted sample with encapsulation size E3 showed the poorest performance of all, achieving only a 76% success rate, with a 24% failure rate. This significant reduction in durability suggested that the combination of a knitted fabric structure and E3 encapsulation may not provide sufficient protection for e-yarns under the strain of repeated washing.

Overall, the integration technique appeared to have the greatest influence on wash durability, as embroidered fabrics consistently outperformed the other integration techniques, maintaining nearly perfect wash durability across all encapsulation sizes, except for a minor 2.8% failure rate for E1.5. Woven fabrics, while exhibiting high durability in most scenarios, demonstrated noticeable failure rates in E2 and E3. Although successful in certain instances, integrated-knit samples showed the highest failure rates, particularly in E3 and E6, highlighting their relative vulnerability compared to woven and embroidered alternatives. These results differ from earlier work, which suggested that the micro-pod size might have an influence on the wash durability of the e-textiles [26]. However, it is possible that such a trend might emerge if the samples were tested to failure. Given the low rate of failure, it is possible that there was no systematic trend in the failures observed and further analysis of the failure mechanism was necessary. Additionally, Figures A3–A7 (Appendix B), illustrate the average resistance values for samples created using each encapsulation size across the 25 wash cycles. The full dataset of individual sample functionality analyses after each wash cycle is also available in the data archive on Figshare.

3.2. Analysis of Failed Samples

The analysis of failed samples after 25 washing cycles provides valuable insights into the potential failure mechanisms and highlights areas for improvement in both manufacturing and encapsulation techniques. Each of the samples that did not survive 25 wash cycles, E2-1W, E3-1W, E3-1K, E3-4K, E6-6E, E1.5-10E, and E1.5-6K, demonstrated distinct electrical continuity or mechanical durability issues.

The samples E2-1W and E1.5-10E exhibited electrical failure at the soldering contact point, first observed during the 6th and 18th wash cycles, respectively. Closer examination revealed that applying pressure to the encapsulated area temporarily restored functionality, indicating that the failure was likely due to a weak solder joint. This suggests that the issue may have originated from poor soldering quality, or the presence of air bubbles trapped during encapsulation, compromising the integrity of the electrical connection over repeated wash cycles. Radiography further confirmed this observation, revealing defects at

the soldering joint, as shown in Figure 6. These results highlight the need for optimized manufacturing processes and encapsulation techniques to ensure the long-term durability and performance of e-yarns in wearable applications.

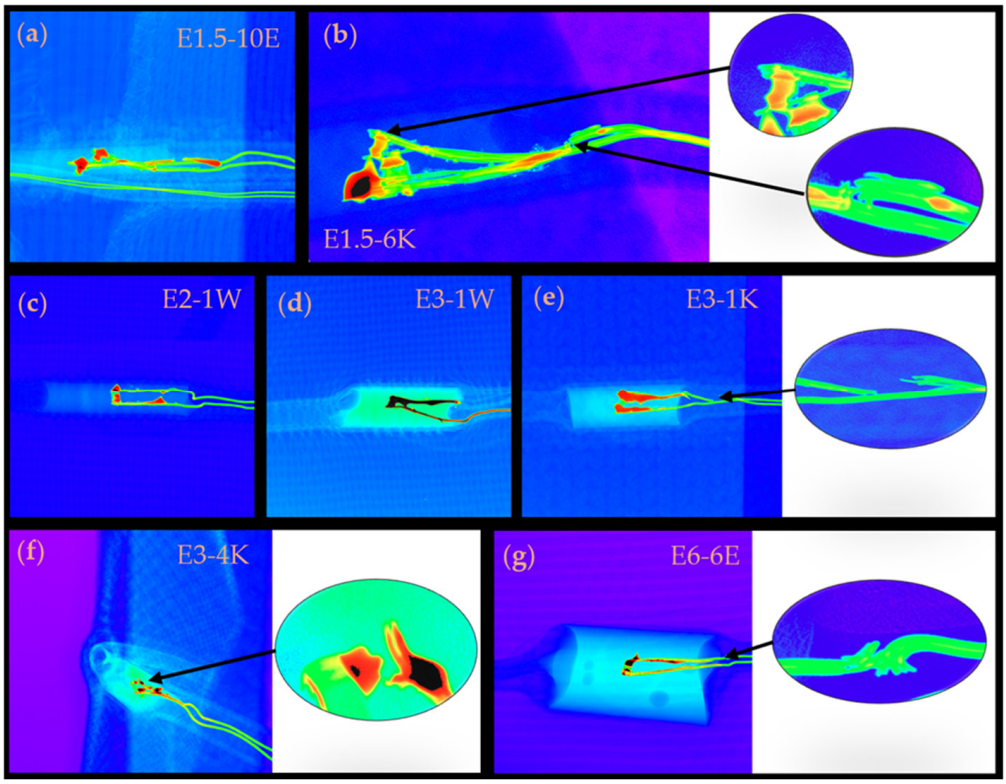

Figure 6. Radiographs of samples where breakages occurred; for contrast, the greyscale has been converted to a spectrum scale in which white/purple represents low absorption and red/black represents high X-ray absorption. Insert images have been used to magnify areas where breakages have occurred. (**a**) Sample E1.5-10E; (**b**) Sample E1.5-6K; (**c**) Sample E2-1W; (**d**) Sample E3-1W; (**e**) Sample E3-1K; (**f**) Sample E3-4K; (**g**) Sample E6-6E.

In the cases of E3-1W, E3-1K, and E6-6E, the failure was attributed to litz wire breakage, as illustrated in Figures 5 and 6. Notably, in E3-1W, the breakage occurred precisely at the point where the wire exited the encapsulation area, suggesting a potential weakness introduced at the interface between the encapsulated and the exposed wire. Importantly, the increased density observed in the radiographs suggested the presence of solder at this interface. Solder significantly increased the rigidity of the litz wire, which would make it more susceptible to breakages due to external mechanical stresses, such as twisting, flexing, or repeated strain during washing.

For E3-1K and E6-6E, potential contributing factors may have included manufacturing inconsistencies or defects at the factory level in the litz wire itself that could have compromised its durability under mechanical loading. It has also been noted that knotting of the litz wire weakens the structure; if a knot had formed, this may have led to the observed failures. However, it is crucial to emphasize that this failure mode was relatively rare, with only four occurrences out of 90 samples, resulting in a low failure rate of 4.4%. This indicates that, despite these isolated incidents, the overall reliability of the litz wire remains high.

In the case of E1.5-6K, the failure was attributed to both litz wire breakage and electrical failure at the soldering contact point, which was observed at the 13th wash cycle. The litz wire breakage suggested that mechanical stress, potentially exacerbated by repeated flexing during washing, contributed to the failure. Additionally, the electrical failure at

the soldering joint may have resulted from manufacturing defects, such as poor solder adhesion or the presence of air bubbles within the encapsulation. These findings highlight the need for further investigation into solder joints' durability and the mechanical resilience of encapsulated litz wire under repeated washing conditions.

Sample E3-4K experienced electrical failure due to a poor solder joint, which caused the detachment of the wire from the component during the first wash cycle. This early failure suggests that the soldering quality was insufficient, potentially due to improper bonding during assembly and a poor-quality encapsulation. The detachment at such an early stage indicates that the joint lacked the necessary mechanical strength to withstand even minimal mechanical stress.

Critically, this analysis identified that of the seven failures, five were due to manufacturing defects, with only two of the ninety samples breaking due to a reason that was not clearly identified as a manufacturing defect.

The image below (Figure 7) shows a sample with an enlarged view of the breakage zone, clearly highlighting the structural damage and failure points resulting from mechanical stress.

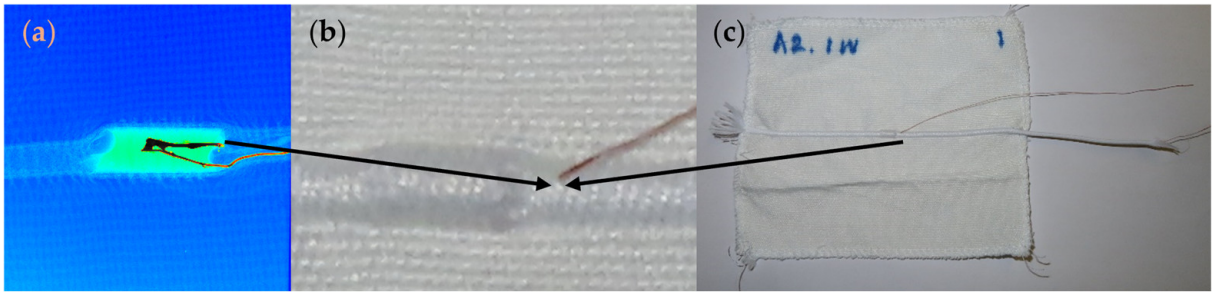

Figure 7. E3-1W sample shown in (**a**) X-ray radiograph revealing internal damage, (**b**) close-up of breakage zone, and (**c**) full sample view.

4. Conclusions

This work provides a useful case study on electronic textile wash durability. The work explored the durability of e-yarns constructed using different encapsulation sizes and integrated into textiles with different techniques. Overall, the wash durability of the e-yarns was good, showing the longevity and reliability of e-yarns, and therefore their suitability for real-world applications. Smaller encapsulation sizes, such as 1.5 mm (E1.5 and E1.5-P), consistently demonstrated superior performance across different fabric types. Woven and embroidered fabrics achieved perfect durability rates, while knitted fabrics achieved a high success rate ranging from 94% to 100%.

While the authors believe that the failures can largely be attributed to manufacturing defects, it is possible that the integration method and micro-pod size may have contributed to the failures observed. This is most noticeable in the woven and knitted fabrics, which performed more variably than the embroidered fabric. It was shown that the embroidered fabrics were somewhat more susceptible to variations in procedures, possibly indicating a need for closer controls during the embroidery process.

In contrast, larger encapsulation sizes, like E3 and E6, may have exhibited weaknesses with certain fabrics, especially integrated-knit textiles. For example, the E3 encapsulation size resulted in a 24% failure rate in knitted fabrics, likely due to structural limitations and bending during washing. Conversely, woven and embroidered fabrics demonstrated resilience to larger encapsulation sizes, with the E6 achieving 100% durability. These findings emphasize the necessity of customizing encapsulation dimensions to align with specific integration methods and fabric types to preserve durability. The practical implications of these findings highlight the necessity of optimizing encapsulation methods to ensure

that e-yarns maintain their functionality and withstand repeated washing, making them suitable for everyday wear. Smaller encapsulations help mitigate stress-induced failures in flexible fabrics like knits, while larger sizes enhance durability in more rigid fabrics like woven textiles.

Finally, an analysis of 90 samples subjected to 25 wash cycles revealed a low failure rate of only 7.8%, with seven failures recorded. Of the samples that broke, five are known to have broken due to manufacturing defects. This outcome indicates the overall reliability of the materials and manufacturing processes involved. Identifying failure mechanisms such as poor solder joints (manufacturing-related), litz wire breakage, and mechanical stresses offers valuable insights for future enhancements. Subsequent research will aim to improve encapsulation techniques, optimize soldering quality, and enhance litz wire durability to minimize failure rates and ensure the long-lasting performance of electronic yarns in wearable applications. It is believed that superior durability can be achieved by removing the error intrinsic to manually conducted soldering and encapsulation processes, and future wash tests will be conducted using e-yarns produced using an automated production process. By addressing these challenges, this research contributes to the development of smart textiles that are more durable and commercially viable, reinforcing their practicality for real-world use.

For optimal integration, it is crucial to tailor the electronic component packaging size to the specific application. In ergonomic wearables, a context in which user comfort is key, smaller packages are vital, so the smallest possible micro-pod is desired. This work, however, does not indicate that a larger encapsulation improves durability. While larger packages may still be necessary for some applications where larger incorporated components are needed, such as industrial textiles, protective gear, or robotics, in these cases comfort during prolonged wear is less important than performance and resilience. By taking an application-specific approach, both functionality and user acceptance can be ensured.

The electronics incorporation technique used in this work differs from more conventional techniques in which electronics are appended to complete textiles using processes such as printing [40], which has resulted in significant research into the improvement of protective planar encapsulation for application on textiles, and reported in recent review articles [41,42]. While that work is less relevant to the type of electronic textile tested here, it may hold relevance to other fiber and yarn-type e-textiles [1,8,28] in which conformable encapsulations over yarn and fiber-like structures are used to improve wash durability [5,41].

Emerging environmental and safety concerns regarding the washing of e-textiles should also be considered, particularly relating to the wash-induced release of conductive or potentially hazardous substances into wastewater systems. Recent studies have shown that components such as metallic fibers, conductive inks, and nanomaterials used in e-textiles may pose toxicological risks comparable to those found in broader e-waste streams [15,42]. These materials can leach into water during laundering, potentially impacting aquatic ecosystems and raising concerns about long-term accumulation and human exposure. To mitigate these risks, there is a growing need to explore sustainable and biodegradable alternatives to conventional conductive materials [15], alongside designing products for end-of-life recyclability and reduced environmental impact. However, implementing these solutions remains challenging due to the lack of standardized wash-testing protocols and the complex interactions between textile structures, detergents, and washing conditions [43]. Consequently, future research should focus on integrated approaches that combine materials science, environmental toxicology, and policy development. Adopting a circular design perspective that addresses safety across the entire product lifecycle will be

essential to minimizing ecological harm while preserving the functional benefits of e-textile technologies [42].

Author Contributions: Conceptualization, A.M.S., T.D. and T.H.-R.; methodology, A.M.S., D.E.-C. and T.H.-R.; formal analysis, A.M.S.; investigation, A.M.S., P.E., T.P., K.M., D.E.-C. and Z.R.; resources, P.E., K.M., T.P. and C.O.; data curation, A.M.S., P.E. and Z.R.; writing—original draft preparation, A.M.S.; writing—review and editing, A.M.S., P.E., K.M., T.P., C.O., Z.R., T.D., D.E.-C. and T.H.-R.; visualization, A.M.S., P.E., K.M. and T.H.-R.; supervision, A.M.S. and T.H.-R.; funding acquisition, T.D. and T.H.-R. All authors have read and agreed to the published version of the manuscript.

Funding: This research was funded by the Engineering and Physical Sciences Research Council (EPSRC) grant EP/T001313/1 Production engineering research for the manufacture of novel electronically functional yarns for multifunctional smart textiles.

Data Availability Statement: Data are contained within the article. The raw datasets used for this work can also be found on Figshare at https://doi.org/10.6084/m9.figshare.28937171 (accessed on 5 May 2025).

Acknowledgments: The authors express their gratitude to Malindu Ehelagasthenna, Abi Smith, and Matholo Scott for their valuable assistance and support in this research. The authors would also like to thank the Imaging Suite at the Medical Technologies Innovation Facility (MTIF) for providing facilities in support of this research.

Conflicts of Interest: The authors declare no conflict of interest.

Appendix A

Comparison of Fabric Thickness and Weight Before and After E-Yarn Integration

Figures A1 and A2 present a comparison between the base fabrics and those integrated with e-yarns, in terms of both thickness and weight. It can be observed that the integration of e-yarns leads to a noticeable increase in fabric thickness and overall weight. Also, a detailed summary of the measured thickness and weight values for each base textile, with and without e-yarn integration, is provided in the accompanying Table A1, offering a clearer understanding of the extent to which integration affects the dimensional properties of the textiles.

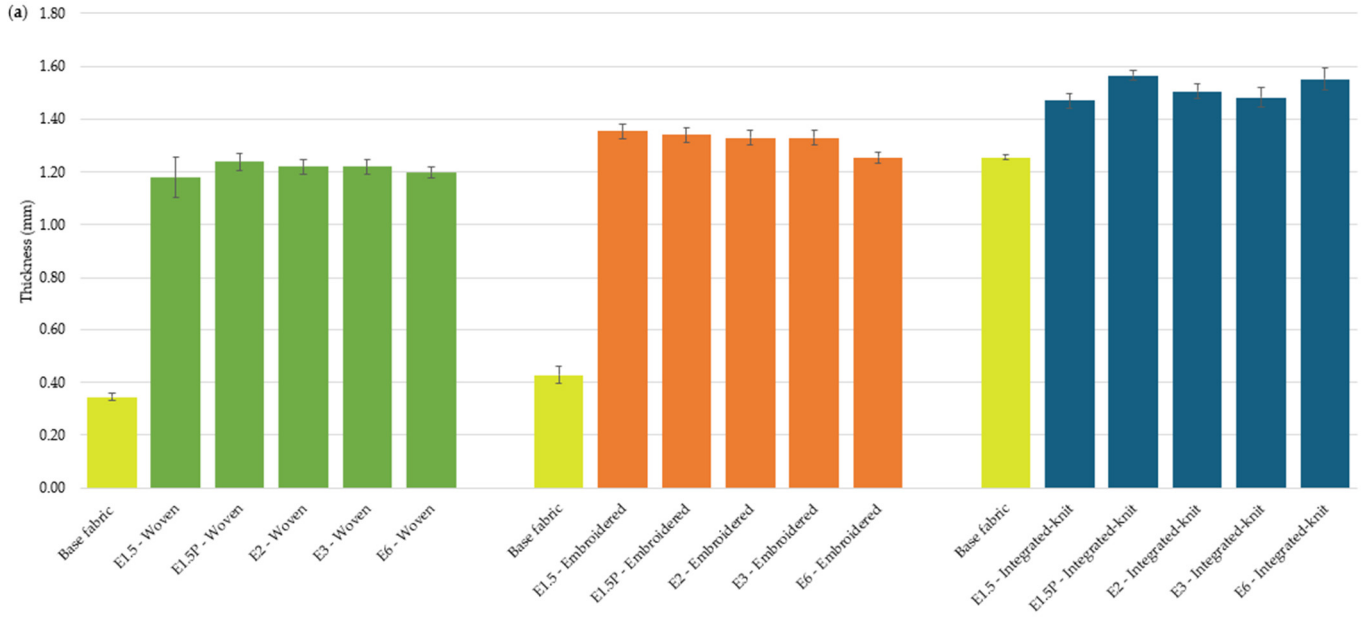

Figure A1. *Cont.*

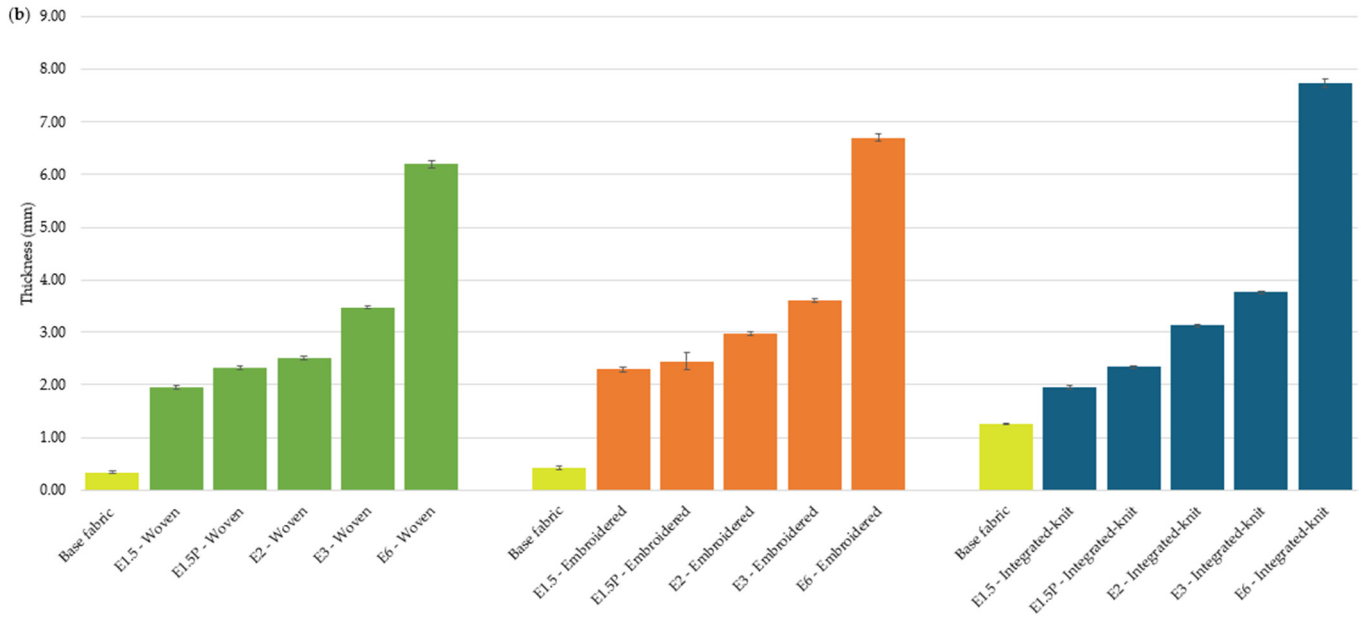

Figure A1. Comparison of base fabric thickness relative to the integrated fabrics. Results using different fabric integration techniques, namely, woven, embroidered, and integrated-knit, and for encapsulation sizes (E1.5, E1.5P, E2, E3, and E6) are shown. Error bars indicate measurement variability. (**a**) Comparison of the base fabrics with no integrated component. (**b**) Comparison following the integration of the electronic yarn at the textile's thickest point.

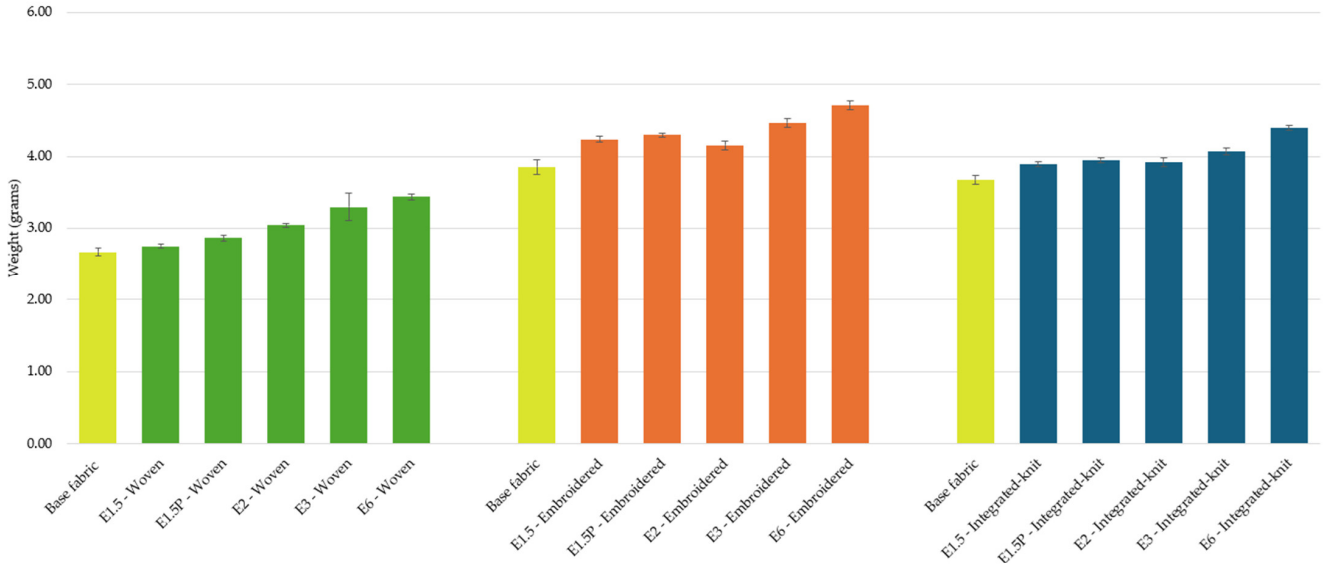

Figure A2. Comparison of base fabric weights and the e-yarn-integrated fabrics' weights. Results using different fabric integration techniques, namely, woven, embroidered, and integrated-knit, and for varying encapsulation sizes (E1.5, E1.5P, E2, E3, and E6) are shown. Error bars indicate measurement variability.

A summary of the thicknesses and weights of the base textiles is provided in Table A1.

Table A1. Fabric thickness and weight information.

Base Fabric	Thickness (mm)	Weight (g)
Woven	0.34 ± 0.01	2.67 ± 0.05
Embroidered	0.43 ± 0.03	3.86 ± 0.1
Integrated-Knit	1.26 ± 0.01	3.67 ± 0.06

Appendix B

Resistance Values Across 25 Wash Cycles

Figures A3–A7 illustrate the resistance values measured over 25 wash cycles for samples produced using various encapsulation sizes. The average values for each sample across these cycles are shown. For samples that failed before completing all 25 cycles, the average resistance was calculated only up to the point of failure. This approach ensures a fair representation of durability and consistent electrical performance across the samples, as characterized by different encapsulation sizes and samples, during washing.

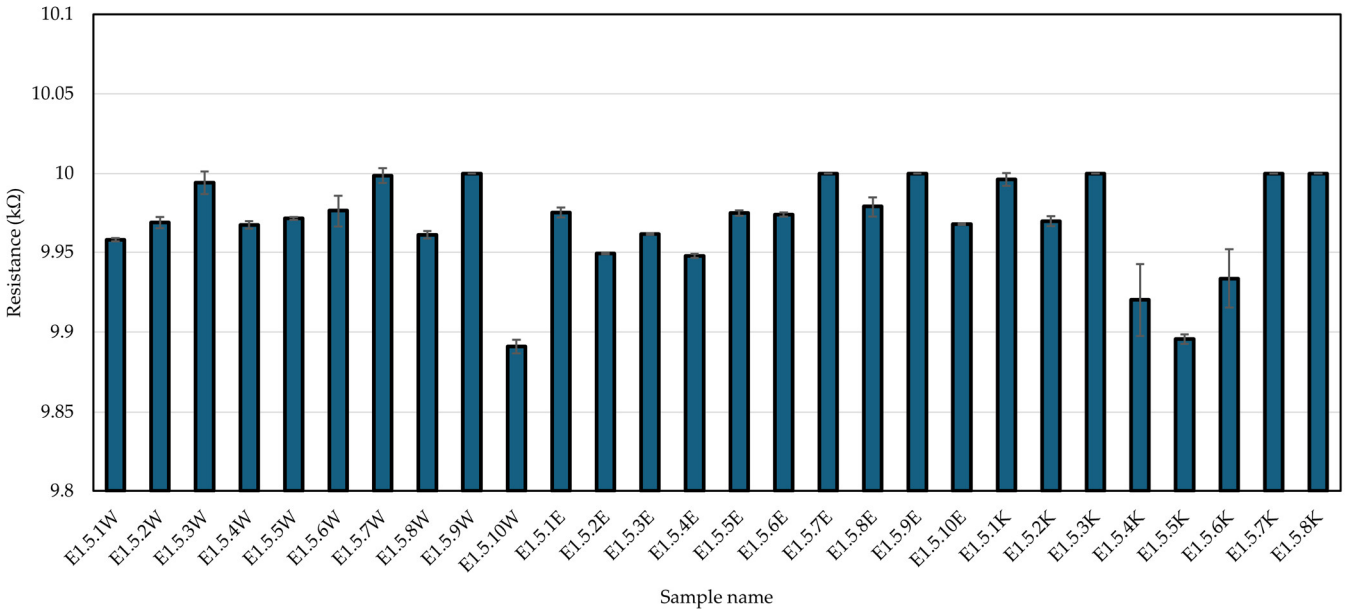

Figure A3. The average resistance values for samples tested over 25 wash cycles, made using an encapsulation size of 1.5 mm (E1.5), across three different integration techniques: woven, embroidered, and integrated-knit. Notably, sample E1.5.10E (embroidered) failed at the 19th wash cycle, and sample E1.5.5K (integrated-knit) failed at the 14th wash cycle. For these samples, the average resistance was calculated only up to the point of failure, to ensure accurate representation of their performance.

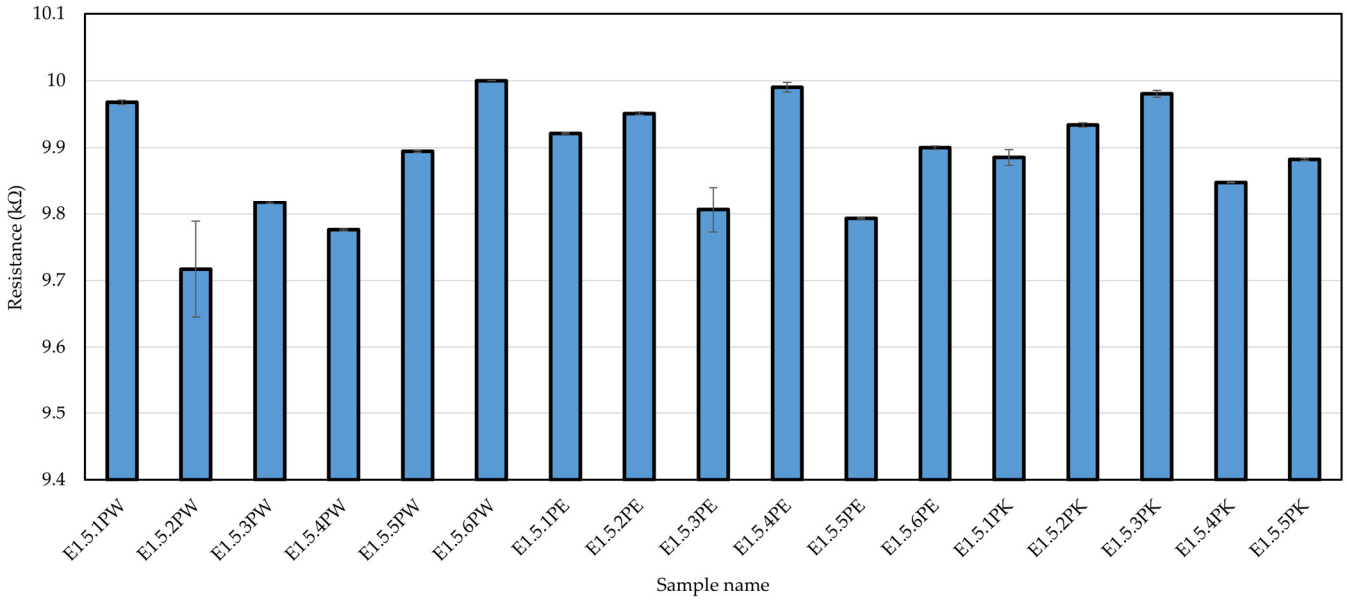

Figure A4. The average resistance values for samples, tested over 25 wash cycles, made using an encapsulation size of 1.5 mm (E1.5P) across three different integration techniques: woven, embroidered, and integrated-knit. Notably, no failure was detected.

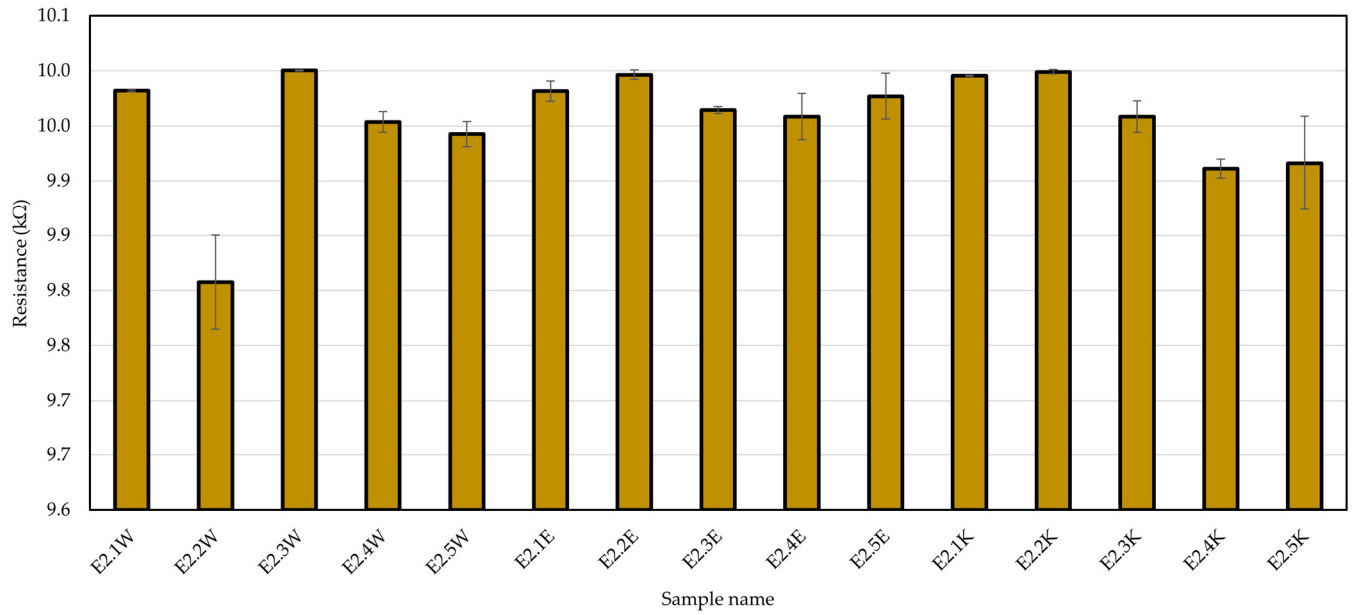

Figure A5. The average resistance values for samples, tested over 25 wash cycles, made using an encapsulation size of 2 mm (E2) across three different integration techniques: woven, embroidered, and integrated-knit. Notably, sample E2.1W (woven) failed at the 7th wash cycle, For this sample, the average resistance was calculated only up to the point of failure, to ensure an accurate representation of their performance.

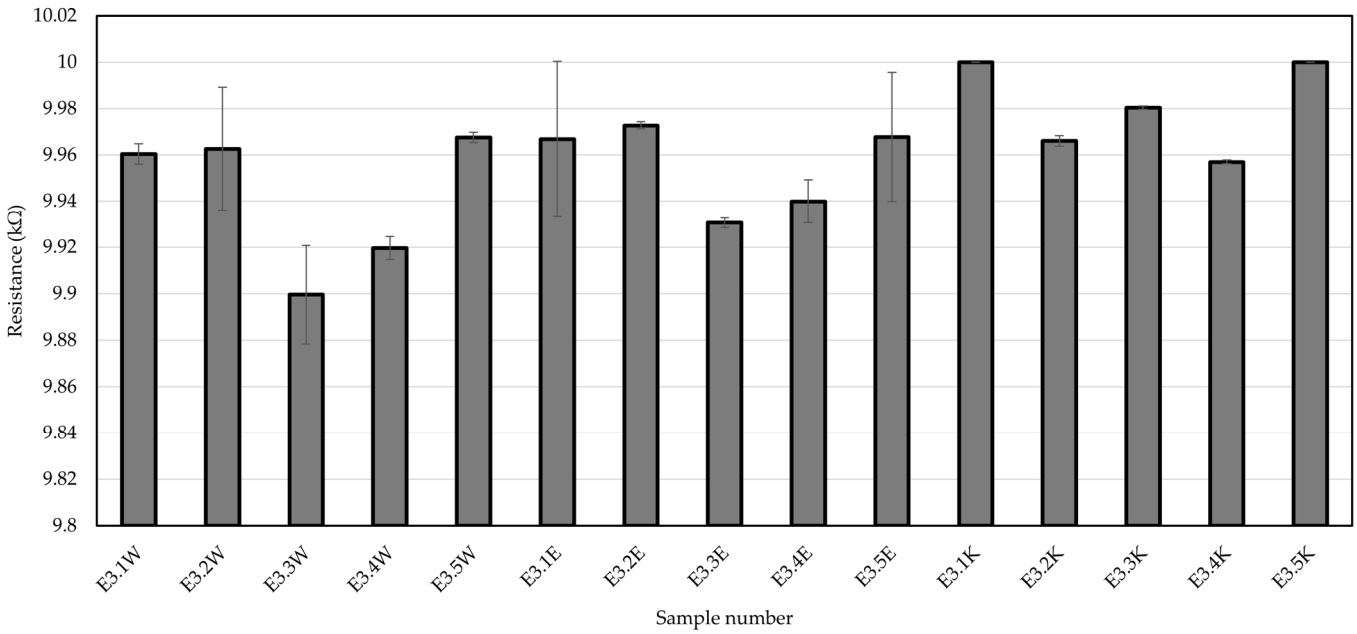

Figure A6. The average resistance values for samples, tested over 25 wash cycles, made using an encapsulation size of 3 mm (E3) across three different integration techniques: woven, embroidered, and integrated-knit. Notably, sample E3.1W (Woven) failed at the 6th wash cycle, sample E3.1K (integrated-knit) failed at the 19th wash cycle, and sample E3.4K (integrated-knit) failed at the 2nd wash cycle. For these samples, the average resistance was calculated only up to the point of failure, to ensure accurate representation of their performance.

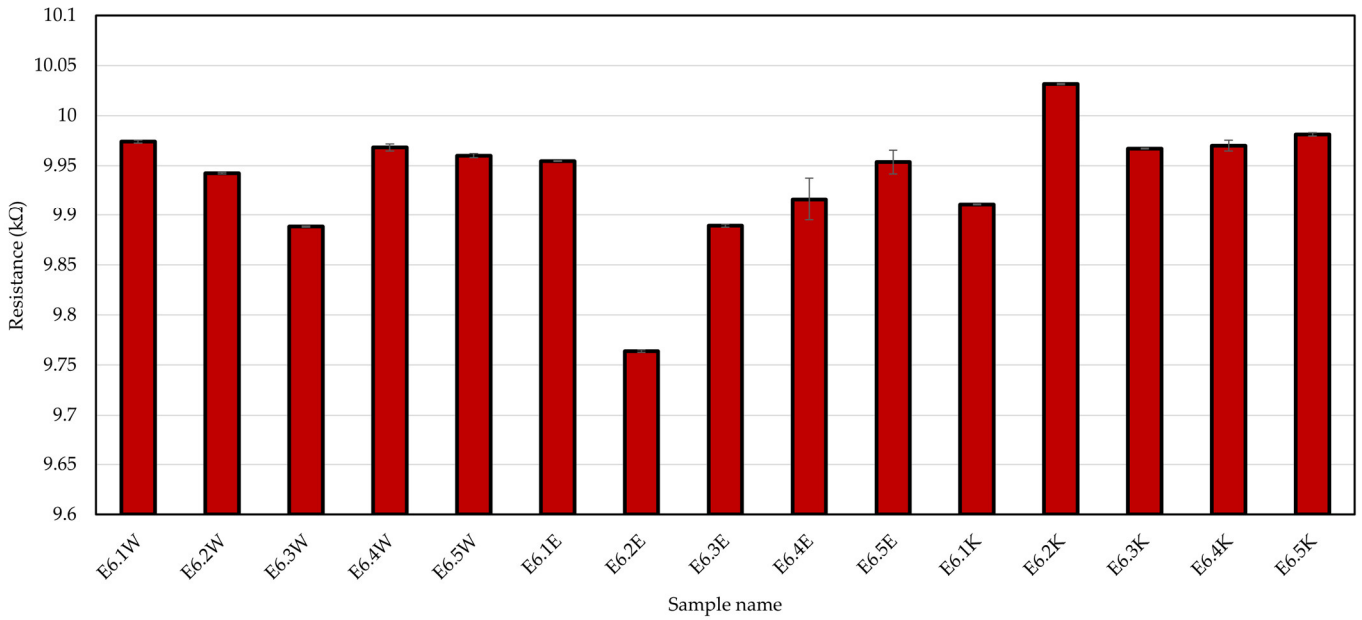

Figure A7. The average resistance for samples, tested over 25 wash cycles, made using an encapsulation size of 6 mm (E6) across three different integration techniques: woven, embroidered, and integrated-knit. Notably, sample E6.5E (embroidered) failed at the 11th wash cycle, For this sample, the average resistance was calculated only up to the point of failure, to ensure accurate representation of its performance.

References

1. Lam, N.Y.K.; Tan, J.; Toomey, A.; Cheuk, K.C.J. Washability and abrasion resistance of illuminative knitted e-textiles with POFs and silver-coated conductive yarns. *Fash. Text.* **2022**, *9*, 39. [CrossRef]
2. Rotzler, S.; von Krshiwoblozki, M.; Kallmayer, C.; Schneider-Ramelow, M. Washability of e-textiles: Washing behavior of textile integrated circuits depending on textile substrate, circuit material and integration method. *Adv. Funct. Mater.* **2024**, *35*, 2417344. [CrossRef]
3. Rotzler, S.; von Krshiwoblozki, M.; Schneider-Ramelow, M. Washability of e-textiles: Current testing practices and the need for standardization. *Text. Res. J.* **2021**, *91*, 2401–2417. [CrossRef]
4. Younes, B. Smart e-textiles: A review of their aspects and applications. *J. Ind. Text.* **2023**, *53*, 1–23. [CrossRef]
5. Zhang, Y.; Wang, H.; Lu, H.; Li, S.; Zhang, Y. Electronic fibers and textiles: Recent progress and perspective. *iScience* **2021**, *24*, 102716. [CrossRef]
6. Meena, J.S.; Choi, S.B.; Jung, S.-B.; Kim, J.-W. Electronic textiles: New age of wearable technology for healthcare and fitness solutions. *Mater. Today Bio* **2023**, *19*, 100575. [CrossRef]
7. Komolafe, A.; Zaghari, B.; Torah, R.; Weddell, A.S.; Khanbareh, H.; Tsikriteas, Z.M.; Vousden, M.; Wagih, M.; Jurado, U.T.; Shi, J.; et al. E-textile technology review—From materials to application. *IEEE Access* **2021**, *9*, 97152–97179. [CrossRef]
8. Rotzler, S.; Schneider-Ramelow, M. Washability of e-textiles: Failure modes and influences on washing reliability. *Textiles* **2021**, *1*, 37–54. [CrossRef]
9. Cherenack, K.; van Pieterson, L. Smart textiles: Challenges and opportunities. *J. Appl. Phys.* **2012**, *112*, 091301. [CrossRef]
10. uz Zaman, S.; Tao, X.; Cochrane, C.; Koncar, V. Launderability of conductive polymer yarns used for connections of e-textile modules: Mechanical stresses. *Fibers Polym.* **2019**, *20*, 2362–2373. [CrossRef]
11. Ojstršek, A.; Plohl, O.; Gorgieva, S.; Kurečič, M.; Jančič, U.; Hribernik, S.; Fakin, D. Metallisation of textiles and protection of conductive layers: An overview of application techniques. *Sensors* **2021**, *21*, 3508. [CrossRef]
12. Liman, M.L.R.; Islam, M.T. Emerging washable textronics for imminent e-waste mitigation: Strategies, reliability, and perspectives. *J. Mater. Chem. A* **2022**, *10*, 1004–1045. [CrossRef]
13. Du, K.; Lin, R.; Yin, L.; Ho, J.S.; Wang, J.; Lim, C.T. Electronic textiles for energy, sensing, and communication. *iScience* **2022**, *25*, 104028. [CrossRef] [PubMed]
14. Chatterjee, K.; Tabor, J.; Ghosh, T.K. Electrically conductive coatings for fiber-based e-textiles. *Fibers* **2019**, *7*, 51. [CrossRef]
15. Dulal, M.; Afroj, S.; Ahn, J.; Cho, Y.; Carr, C.; Kim, I.D.; Karim, N. Toward sustainable wearable electronic textiles. *ACS Nano* **2022**, *16*, 19755–19788. [CrossRef]

16. Hossain, M.M.; Bradford, P.D. Durability of smart electronic textiles. In *Nanosensors and Nanodevices for Smart Multifunctional Textiles*; Elsevier: Amsterdam, The Netherlands, 2021; pp. 27–53. [CrossRef]
17. Wu, B.; Zhang, B.; Wu, J.; Wang, Z.; Ma, H.; Yu, M.; Li, L.; Li, J. Electrical switchability and dry-wash durability of conductive textiles. *Sci. Rep.* **2015**, *5*, 11255. [CrossRef]
18. Rahemtulla, Z.; Hughes-Riley, T. The Design and Engineering of a Fall Detection Electronic Textile. 2023. Available online: https://figshare.com/articles/dataset/The_design_and_engineering_of_a_fall_detection_electronic_textile/21632078/1 (accessed on 31 January 2023).
19. Rahemtulla, Z.; Wickenden, R.; Hughes-Riley, T. Using a human centred design approach to develop a fall detection sock for older women. *Des. Health* **2024**, *8*, 318–335. [CrossRef]
20. Ebrahimi, P.; Shahidi, A.M.; Koutsogeorgis, D.; Oliveira, C.; Kaner, J.; Dias, T.; Hughes-Riley, T. Further optimization of solar electronic yarns for developing large, stretchable knitted textile solar panels. In Proceedings of the 2024 International Conference on Challenges, Opportunities, Innovations and Applications in Electronic Textiles (E-Textiles), Berlin, Germany, 19–21 November 2024; pp. 58–66.
21. Shahidi, A.M.; Marasinghe, K.; Ebrahimi, P.; Oliveira, C.; Perera, N.; Briggs-Goode, A.; Dias, T.; Hughes-Riley, T. Design considerations for the creation of electronic yarns for wearable health monitoring devices. *Des. J.* **2025**, *28*, 432–451. [CrossRef]
22. Blecha, T.; Hirman, M.; Navrátil, J. Assembly technology of electronic components for e-textiles. *Power Electron. Devices Compon.* **2024**, *7*, 100056. [CrossRef]
23. Hughes-Riley, T.; Dias, T.; Cork, C. A historical review of the development of electronic textiles. *Fibers* **2018**, *6*, 34. [CrossRef]
24. Nashed, M.N.; Hardy, D.A.; Hughes-Riley, T.; Dias, T. A novel method for embedding semiconductor dies within textile yarn to create electronic textiles. *Fibers* **2019**, *7*, 12. [CrossRef]
25. Hardy, D.A.; Rahemtulla, Z.; Satharasinghe, A.; Shahidi, A.; Oliveira, C.; Anastasopoulos, I.; Nashed, M.N.; Kgatuke, M.; Komolafe, A.; Torah, R.; et al. Wash testing of electronic yarn. *Materials* **2020**, *13*, 1228. [CrossRef] [PubMed]
26. Simegnaw, A.A.; Malengier, B.; Rotich, G.; Tadesse, M.G.; van Langenhove, L. Review on the integration of microelectronics for e-textile. *Materials* **2021**, *14*, 5113. [CrossRef] [PubMed]
27. Shak Sadi, M.; Kumpikaitė, E. Advances in the robustness of wearable electronic textiles: Strategies, stability, washability and perspective. *Nanomaterials* **2022**, *12*, 2039. [CrossRef]
28. *BS EN ISO 6330:2021*; Textiles—Domestic Washing and Drying Procedures for Textile Testing. International Organization for Standardization: Geneva, Switzerland, 2021.
29. Rotzler, S.; Kallmayer, C.; Dils, C.; von Krshiwoblozki, M.; Bauer, U.; Schneider-Ramelow, M. Improving the washability of smart textiles: Influence of different washing conditions on textile integrated conductor tracks. *J. Text. Inst.* **2020**, *111*, 1762–1773. [CrossRef]
30. Ankhili, A.; Tao, X.; Cochrane, C.; Coulon, D.; Koncar, V. Washable and reliable textile electrodes embedded into underwear fabric for electrocardiography (ECG) monitoring. *Materials* **2018**, *11*, 256. [CrossRef] [PubMed]
31. Kazani, I.; Declercq, F.; Scarpello, M.L.; Hertleer, C.; Rogier, H.; Ginste, D.V.; Mey, G.D.; Guxho, G.; van Langenhove, L. Performance study of screen-printed textile antennas after repeated washing. *AUTEX Res. J.* **2014**, *14*, 47–54. [CrossRef]
32. Baribina, N.; Baltina, I.; Oks, A. Application of additional coating for conductive yarns protection against washing. *Key Eng. Mater.* **2018**, *762*, 312–317. [CrossRef]
33. Tadesse, M.G.; Mengistie, D.A.; Chen, Y.; Wang, L.; Loghin, C.; Nierstrasz, V. Electrically conductive highly elastic polyamide/lycra fabric treated with PEDOT:PSS and polyurethane. *J. Mater. Sci.* **2019**, *54*, 9591–9602. [CrossRef]
34. Dils, C.; Hohner, S.; Schneider-Ramelow, M. Use of rotary ultrasonic plastic welding as a continuous interconnection technology for large-area e-textiles. *Textiles* **2023**, *3*, 66–87. [CrossRef]
35. Liu, X.; Zhang, D.; Qiu, H.; Sun, J.; Mao, C.; Qian, K. On-axis fatigue behaviors and failure characterization of 3D5D braided composites with yarn-reduction using X-ray computed tomography. *Compos. Sci. Technol.* **2021**, *203*, 108585. [CrossRef]
36. Cao, W.; Zhang, J.; Sun, B.; Gu, B. X-ray tomography and numerical study on low-velocity impact damages of three-dimensional angle-interlock woven composites. *Compos. Struct.* **2019**, *230*, 111525. [CrossRef]
37. Tao, X.; Koncar, V.; Huang, T.-H.; Shen, C.-L.; Ko, Y.-C.; Jou, G.-T. How to make reliable, washable, and wearable textronic devices. *Sensors* **2017**, *17*, 673. [CrossRef] [PubMed]
38. Islam, M.R.; Afroj, S.; Yin, J.; Novoselov, K.S.; Chen, J.; Karim, N. Advances in printed electronic textiles. *Adv. Sci.* **2024**, *11*, 2304140. [CrossRef] [PubMed]
39. Ghosh, J.; Rupanty, N.S.; Noor, T.; Asif, T.R.; Islam, T.; Reukov, V. Functional coatings for textiles: Advancements in flame resistance, antimicrobial defense, and self-cleaning performance. *RSC Adv.* **2025**, *15*, 10984–11022. [CrossRef] [PubMed]
40. Amarnath, M.; Mohite, S.; Palaskar, S. Recent advances and innovations in textile materials for smart sensor applications: A review. *Measurement* **2025**, *255*, 118057. [CrossRef]
41. Wicaksono, I.; Tucker, C.I.; Sun, T.; Guerrero, C.A.; Liu, C.; Woo, W.M.; Pence, E.J.; Dagdeviren, C. A tailored, electronic textile conformable suit for large-scale spatiotemporal physiological sensing in vivo. *npj Flex. Electron.* **2020**, *4*, 5. [CrossRef]

42. Köhler, A.R.; Hilty, L.M.; Bakker, C. Prospective impacts of electronic textiles on recycling and disposal. *J. Ind. Ecol.* **2011**, *15*, 496–511. [CrossRef]
43. Adamu, M.F.; Tesfaye, T.; Berhanu, B.; Simegnaw, A.A. Electronic textiles. *Text. Prog.* **2025**, *57*, 1–71. [CrossRef]